ANN Based Detection and Location of Severe Three Phase Trip on the Transmission Lines of an Uncontrolled Power System

Muntaser Abdulwahid Salman
M.Sc. Electrical engineering
Computer College
Al-Anbar University

Suhail Muhammad Ali
M.Sc. Electrical engineering
Computer College
Al-Anbar University

Abstract

Severe three phase trips are simulated on four arbitrary locations of an uncontrolled power system transmission lines. The responses of three measurable state variables of the system (rotor speed, stator direct axis current, and stator quadrature - axis current) are recorded, and suitable ANNs are trained to detect and locate the positions of the corresponding trips. The paper proves that this method is quick, active and accurate to diagnose and find the locations of that kind of trips.

Key Words: ANN, detection, three phase trip, transmission line, power system.

1. Introduction

An overhead transmission line (TL) is one of the main components in every electrical power system. The transmission line is exposed to the environment and the possibility of experiencing faults on the transmission line is generally higher than that on other main components. Line faults are the most common faults, they may be triggered by lightning strokes, trees may fall across lines, fog and salt spray on dirty insulators may cause the insulator strings to flash over, and ice and snow loadings may cause insulator strings to fail mechanically. When a fault occurs on an electrical transmission line, it is very important to detect it and to find its location in order to make necessary repairs and to restore power as soon as possible. The time needed to determine the fault point along the line will affect the quality of the power delivery [1].

The growing demand for power supply and high transmission efficiencies has prompted construction of extra high voltage transmission lines. These high voltage lines have become the backbone of the bulk power transmission over long distances. The complexity of the power network and the low stability margins at which they now operate have dramatically increased the occurrence of catastrophic failures in electric power system [2]. Although complete immunity from such catastrophic failure is not easy to achieve, new developments in the transmission lines protection show promising signs that cascading system outages can be minimized and mitigated. The greatest danger to a healthy power system is instability resulting from faults that are not cleared quickly. High speed fault isolation is required to insure that the power system (PS) will not run into transient stability problems [2].

2. Literature Survey

Fault location in transmission lines has been a subject of interest for many years. During the last decade a number of fault location algorithms have been developed, including the steady-state phasor approach, the differential equation approach and the traveling-wave approach, as well as two-end and one-end algorithms. In the last category, synchronized and non-synchronized sampling techniques are used [1]. However, two-terminal data are not

widely available. From a practical viewpoint, it is desirable for equipment to use only one terminal data. The one-end algorithms, in turn, utilize different assumptions to replace the remote end measurements. Most of fault locators are only based on local measurements. Currently, the most widely used method of overhead line fault location is to determine the apparent reactance of the line during the time that the fault current is flowing and to convert the ohmic result into a distance based on the parameters of the line. It is widely recognized that this method is subject to errors when the fault resistance is high and the line is fed from both ends, and when parallel circuits exist over only parts of the length of the faulty line [1]. Yann-Chang Huang study [3] presents an adductive reasoning network (ARN) for real-time fault section estimation in electric power systems. The proposed ARN handles complicated and knowledge-embedded relationships between the circuit breaker status (input) and the corresponding candidate fault section (output) using a hierarchical network with several layers of function nodes of simple low-order polynomials. The relay status is then further used to validate the final fault section. Martins et al research,[4] presents a new fault location methodology for electrical power system network using the ($\alpha\beta$) space vector to identify and locate different types of faults. It is based on the modified version of Clarke's transform which is more suitable for real time implementations with invariant power which is known by Clarke – Concordia transformation. Kezunovic et al, [5], develop accurate fault location algorithms for situations where only (sparse field) data is available. The basic concept of matching the recorded and simulated waveforms to determine the most probable fault location is utilized. The recorded waveforms are captured using digital fault recorders while the simulated waveforms are produced by running a short circuit (s/c) program using an accurate model of the PS. This study investigates the feasibility of the new fault location algorithm and proposes possible improvements to it. To determine the degree of matching between recorded and simulated waveforms, during the fault phasor is used to calculate the fitness value. The procedure of finding the best-matched simulation waveform is an optimization problem and solved in this study by a genetic algorithm. Christian et al [6] introduce algorithms for the calculation of the fault level in networks with series compensating FACT devices (FD) conventional methods can not be used because the equivalent series reactance of a converter – based FD depends on the short-circuit current itself, so this paper uses iterative algorithm to stepwise calculate the equivalent reactance and the short-circuit current. Cheong et al paper [7], presents an approach to analyze key characteristics of fault phenomena on a thyristor controlled series capacitor compensated transmission line.

Many successful applications of artificial neural networks (ANNs) to power systems have been demonstrated. Tahar Bouthiba paper [1] deals with the application of artificial neural networks (ANNs) to fault detection and location in extra high voltage (EHV) transmission lines for high speed protection using terminal line data. The proposed neural fault detector and locator were trained using various sets of data available from a selected power network model and simulating different fault scenarios (fault types, fault locations, fault resistances and fault inception angles) and different power system data (source capacities, source voltages, source angles, time constants of the sources). Sanaye-Pasand et al paper [8], presents a novel application of neural network approach to protection of transmission line. Different system faults on a protected transmission line should be detected and classified rapidly and correctly, the paper presents the use of neural networks as a protective relaying pattern classifier algorithm.

3. The Uncontrolled Electrical Power System

Our simple electrical PS is composed of single synchronous generator (SG) of rating (160 MVA ,15KV), and its exciter rating is(345 V ,926 A at rated load),the SG is

connected to an infinite busbar via double circuit long transmission line ,the line voltage is stepped up and down by means of two power transformer (T1 & T2). It is assumed that this simple PS is not controlled (unregulated) by any method of control; this means that the effects of the speed governor and the voltage regulator on the machine transient response (following the disturbance) are not included.

4. PS Mathematical Model

This PS can be represented by state space model consisting of seven first order differential equations as follows:[9]

$$\begin{pmatrix} L_{de} & L_{md} & L_{md} & 0 & 0 & 0 & 0 \\ L_{md} & L_f & L_{md} & 0 & 0 & 0 & 0 \\ L_{md} & L_{md} & L_{kd} & 0 & 0 & 0 & 0 \\ 0 & 0 & 0 & L_{qe} & L_{mq} & 0 & 0 \\ 0 & 0 & 0 & L_{mq} & L_{kq} & 0 & 0 \\ 0 & 0 & 0 & 0 & 0 & \tau_j & 0 \\ 0 & 0 & 0 & 0 & 0 & 0 & 1 \end{pmatrix} \begin{pmatrix} \dot{i}_d \\ \dot{i}_f \\ \dot{i}_{kd} \\ \dot{i}_q \\ \dot{i}_{kq} \\ \dot{\upsilon} \\ \dot{\delta} \end{pmatrix} = \begin{pmatrix} K_1 \sin\delta \\ v_f \\ 0 \\ K_1 \cos\delta \\ 0 \\ T_{mec} \\ -1 \end{pmatrix}$$

$$- \begin{pmatrix} R_{ae} & 0 & 0 & \upsilon L_{qe} & \upsilon L_{mq} & 0 & 0 \\ 0 & r_f & 0 & 0 & 0 & 0 & 0 \\ 0 & 0 & r_{kd} & 0 & 0 & 0 & 0 \\ -\upsilon L_{de} & -\upsilon L_{md} & -\upsilon L_{md} & R_{ae} & 0 & 0 & 0 \\ 0 & 0 & 0 & 0 & r_{kq} & 0 & 0 \\ L_d i_q/3 & L_{md} i_q/3 & L_{md} i_q/3 & -L_q i_d/3 & -L_{mq} i_d/3 & D & 0 \\ 0 & 0 & 0 & 0 & 0 & -1 & 0 \end{pmatrix} \begin{pmatrix} i_d \\ i_f \\ i_{kd} \\ i_q \\ i_{kq} \\ \upsilon \\ \delta \end{pmatrix} \quad (1)$$

Where:

$\mathbf{L_{de} = L_d + L_e}$, $\mathbf{L_{qe} = L_q + L_e}$, $\mathbf{R_{ae} = r_a + R_e}$, $\mathbf{K_1} = \sqrt{3}\ \mathbf{V_\infty}$.[10]

The long transmission line (TL) (longer than 80 Kms) are modeled in this study by an equivalent (π – network) with half of the total capacitor lumped at each end as admittance to neutral (Y/2). (The mutual inductance effects of the double circuit's lines are neglected). The power transformers with off nominal tap ratio (X_{T1} and X_{T2}) are represented by its zero sequence impedances.

5. Computing Procedure Steps

Firstly, the stability mode of the system is tested when applying four arbitrary sets of values of the equivalent resistance (R_{ae}), the equivalent direct –axis inductance (L_{de}) and the equivalent quadrature–axis inductance (L_{qe}) of the system in four steps respectively. **Fig.(1)** shows the distance of these locations from the near end of the transmission line . These four sets of (R_{ae}, L_{de} and L_{qe}) are belonged to the arbitrary four corresponding locations of the heavy three phase short circuit (s/c) trip at the TL. At these four locations a (s/c) trip is simulated and the responses of the (υ), ($\mathbf{i_d}$) and ($\mathbf{i_q}$) are shown in **Figs. (2,3 and 4)**. From these **Figs. , Table** (1) is constructed. In this table the transient values of (υ) , ($\mathbf{i_d}$) and ($\mathbf{i_q}$) that follow the trip -for each case of location - are estimated

6. The Behavior of the PS during and After Subjecting to the Trip

As **Figs. (2, 3** and **4)** show the initial values of (υ) , ($\mathbf{i_d}$) and ($\mathbf{i_q}$) are (1), (-0.25) and (0.5) pu respectively . The disturbance occurs at 0.037 sec and is recovered at 0.71 sec (

lasted for 71.7 micro second duration), the three state variables oscillate around its initial quantities and then settle down at that values after some microseconds.

7. Comments on Figs. (2, 3 and 4) and Table (1)

1: The variations of (υ) , ($\mathbf{i_d}$) and ($\mathbf{i_q}$) seem to be very large in magnitude ,that's because the s/c 3- phase tripe is classified as the worse disturbance case of the PS. Theoretically – as observed from **Fig.(4)** - the speed of the machine rotor for cases (2,3 and 4) become negative , that means: reversing rotating direction (change machine operating mode from generating to motoring) for some microseconds, practically this is impossible due to the moment of inertia of rotor mass.

2: It is noticed that as the location of the s/c fault becomes farer from the near end of the TL ,the modulus of (υ) , ($\mathbf{i_d}$) and ($\mathbf{i_q}$) variations increases , that's because of the increase of (R_{ae}), and decrease of (L_{de} and L_{qe}) of the system , see **Table (3).**

3: Generally, for all of the four cases variation modulus of ($\mathbf{i_d}$ **&** $\mathbf{i_q}$) is larger than that of (υ) (measured in p.u) because as the s/c trip is an electrical disturbance so surely its influence will be clearer on the electrical side than on the mechanical side.

4: For locations (1) and (2) : variation modulus of ($\mathbf{i_q}$) is larger than that of ($\mathbf{i_d}$) whereas for locations (3) and (4): the variation modulus of ($\mathbf{i_d}$) is larger than that of ($\mathbf{i_q}$). The explanation of these phenomena is as follows: when the distance of fault location is small then the reactive effect of the system impedance is greater than the active effect and it follows that: ($\mathbf{i_q}$) is greater than ($\mathbf{i_d}$). The situation is reversed as the fault location distance becomes large.

8. Design Procedure of the ANN Fault Detector and the Fault Locator

The design procedure of the ANN fault detector and the fault locator goes through the following steps:

1. Preparation of a suitable training data set that represents cases the ANN needs to learn.
2. Selection of a suitable ANN structure for a given application.
3. Training the ANN.
4. Evaluation of the trained ANN using test patterns until its performance is satisfactory.

9. Artificial Neural Network

In this paper, the fully-connected multilayer feed-forward neural network (FFNN) was used and trained with a supervised learning algorithm called back-propagation. The FFNN consists of an input layer representing the input data to the network, some hidden layers and an output layer representing the response of the network. Each layer consists of a certain number of neurons; each neuron is connected to other neurons of the previous layer through adaptable synaptic weights *w* and biases b, see **Fig. (5)**.

If the inputs of neuron j are the variables $x_1, x_2, \ldots, x_i, \ldots, x_N$, the output u_j of neuron j is obtained as follows:

$$u_j = \varphi\left(\sum_{i=1}^{N} w_{ij} + b_j\right) \qquad (2)$$

Where w_{ij} represents the weight of the connection between neuron j and the i-th input, b_j represents the bias of neuron j and φ is the transfer function (activation function) of neuron j. An FFNN of three layers (one hidden layer) is considered with N, M and Q neurons for the input, hidden and output layers, respectively. The input patterns of the ANN represented by a vector of variables x = ($x_1, x_2, \ldots, x_i, \ldots, x_N$) submitted to the ANN by the input layer are transferred to the hidden layer. Using the weight of the connection between the input

and the hidden layer, and the bias of the hidden layer, the output vector u = (u_1, u_2, . . . , u_j , . . . , u_M) of the hidden layer is then determined. The output u_j of neuron j is obtained as follows:

$$u_j = \varphi hid\left(\sum_{i=1}^{N} w_{ij}^{hid} + b_j^{hid}\right) \tag{3}$$

Where w_{ij}^{hid} represents the weight of connection between neuron j in the hidden layer and the i-th neuron of the input layer, b_j^{hid} represents the bias of neuron j and φhid is the activation function of the hidden layer. The values of the vector u of the hidden layer are transferred to the output layer. Using the weight of the connection between the hidden and output layers and the bias of the output layer, the output vector y = (y_1, y_2, . . . , y_k, . . . , y_Q) of the output layer is determined. The output y_k of neuron k (of the output layer) is obtained as follows:

$$y_k = \varphi_{out}\left(\sum_{i=1}^{N} w_{jk}^{out} u_j + b_k^{out}\right) \tag{4}$$

Where w_{jk}^{out} represents the weight of the connection between neuron k in the output layer and the j-th neuron of the hidden layer, b_k^{out} represents the bias of neuron k and φ_{out} is the activation function of the output layer. The output y_k (corresponding to the given input vector x) is compared with the desired output (target value) y_k^d. The error in the output layer between y_k and y_k^d (y_k^d - y_k) is minimized using the mean square error at the output layer (which is composed of Q output neurons), defined by :

$$E = \frac{1}{2}\sum_{k=1}^{q}(y_k^d - y_k)^2 \tag{5}$$

The training data set of an ANN should contain the necessary information to generalize the problem. Combinations of different fault conditions were considered and training patterns were generated by simulating different kinds of fault zones on the power system. Fault zones were changed to obtain training patterns covering a wide range of different power system conditions.

10. Fault Detector

10.1 Inputs and Outputs

In order to build up an ANN, the inputs and outputs of the neural network have to be defined for pattern recognition. The inputs to the network should provide a true representation of the situation under consideration. The process of generating input patterns to the ANN fault detector (FD) is depicted from **Figs. (2, 3** and **4)**. The simulated training data set was used to train the ANN-detector is shown in **Table (1)**.

10.2 Structure and Training of the Neural Fault Detector

The fault detection task can be formulated as a pattern classification problem. The fully connected three-layer feed-forward neural network (FFNN) was used to classify faulty/non-faulty data sets and the error back-propagation algorithm was used for training. The numbers of neurons in the input and hidden layers were selected empirically through extensive simulations. Various network configurations were trained and tested in order to establish an appropriate network with satisfactory performances, which were the fault tolerance, time response and generalization capabilities. Once trained, the networks performance was tested using a validation data set. The suitable network which showed satisfactory results was finally selected. Selected network structure is shown in **Fig. (6)** .The network has 3 input neurons and 4 output neurons. The number of neurons for the hidden layer is chosen to be 5 neurons. Based on the fault type which occurs on the system, output neurons should be 0 or 1.

The input layer simply transfers the input vector x to the hidden neurons. The outputs u_j of the hidden layer with the sigmoid activation function are calculated and transferred to the output layer, which is composed of only four neurons. The output value of the neuron in the output layer with the sigmoid activation function calculated gives the state of the transmission line: 1 (the presence of a fault) or 0 (the non-faulty situation).

10.3 Test and Results

Measured currents at the relay location are subject to change when a fault occurs on a transmission line. Fault detection/classification principle may be based upon detecting these changes. The principle of variation of current signals before and after the fault incidence is used and a fast and reliable ANN-based fault detector/classifier module is designed to detect the fault and classify the fault type.

The results - as in **Table (2)** demonstrate the ability of the fault detector to produce a correct response in all simulation tests. The results –**Table (2)** - show the stability of the ANN outputs under normal steady-state conditions and rapid convergence of the output variables to the expected values (either very close to unity or zero) under fault conditions. This clearly confirms the effectiveness of the proposed fault detector. The results show that in the fault cases presented, there is a very rapid transition in the ANN outputs from the pre-fault to the fault states. The results - **Table (2)** - reveal that the neural network is able to generalize the situation from the provided patterns, accurately indicates the presence or the absence of a fault and can be used for on-line fault detection.

11. Fault Locator

11.1 Inputs and Outputs

The ANN fault locator (FL) is to locate faults in our transmission line. The FL is activated when a fault is detected by the fault detector (FD). The ANN forming the FL uses the magnitudes of the R_{ae} , L_{de} and L_{qe} as inputs to the ANN. The output of the ANN fault locator is the estimation of the fault location (in km) in the transmission line, see **Table (3).**

11.2 Structure and Learning Rule of the Neural Fault Locator

A three-layer feed-forward neural network (FFNN) trained using the back propagation algorithm was selected to implement the algorithm for fault location. As regards the ANN structure, parameters such as the number of inputs to the network as well as the neurons in the input and hidden layers were selected empirically. This process involved a trial-and-error procedure with various network configurations which were trained and tested in order to establish the appropriate network with a satisfactory performance.

With supervised learning, the ANN was trained with various input patterns corresponding to different types of fault at various locations for different fault conditions and different power system data. The transfer function of the hidden layer was the sigmoid function and that of the output layer neurons was the linear function. The input layer simply transfers the input vector x to the hidden neurons. The outputs uj of the hidden layer with the sigmoid activation function are calculated and transferred to the output layer, which is composed of only one neuron gives the fault location in the transmission line (in km).

11.3 Test and Results

In the following, we consider the fault classification and only the results for single phase to ground faults which represent the majority (85%) of the faults are presented. To get a good general performance, the fault locators were tested with a set of independent test patterns to cover wide system and fault conditions and different power system data. **Table (3)** contains some test results for fault conditions and power system data. The first column indicates the fault location and the second column on the right indicate the outputs of the ANNs corresponding to the fault locators. The error in fault location is defined as:

$$\text{Error (km)} = |\text{ANN output - Fault location}| \tag{6}$$

Where 'ANN output' is the output (in km) of the ANN fault locator and 'Fault location' is the real distance to the fault in the transmission line (in km). **Table (4)** shows the error in the estimation of the fault location for FL. The criterion for evaluating the performance of the fault locators is defined as:

$$Error(\%) = \frac{|ANN\ Output - Fault\ Locate|}{Length\ of\ the\ line} \tag{7}$$

Test results for fault location are shown in **Table (4).**

12. Conclusions and Future Work

In this paper a new approach to fault detection/phase selection algorithm is presented and its effectiveness is demonstrated. The suggested approach is based on the use of neurocomputing technology and implementation of pattern recognition concepts. The paper presents a positive approach to improve the performance of conventional algorithms. The proposed algorithm is extensively tested by independent test fault patterns and promising results are obtained. Effects of different system parameters and conditions are studied. Extensive studies indicate that the network is able to classify different faults correctly and rapidly and its performance is not affected by the changing network conditions. For future projects, a controlled PS could be studied by including the effects of the speed governor and the voltage regulator on the machine transient response following the s/c disturbance.

References

[1]Tahar Bouthiba, "Fault Location In EHV Transmission Lines Using Artificial Neural Networks," Internal Journal of Application of Mathematical and Computer Science, vol. 14 no. 1. pp 69-78, (2004).

[2] Vajira Pathirana, "A power system protection scheme combining impedance measurement and travelling waves: Software and Hardware implementation," PhD. Thesis, university of Manitoba, Winnipeg, Manitoba, Canada, April, (2004).

[3] Yann-Chang Huang, "A Novel Model for Fault Diagnosis in Electric Power Systems," Department of Electrical Engineering. Cheng Shiu Institute of Technology Kaohsiung, 833, Taiwan, R.O.C.e-mail: huangyc@cc.csit.edu.tw, (2000).
[4] L. Sousa Martins , V. Fernao Pires and C. M. Alegria, "A new Accurate Fault Location Method using αβ Space Vector Algorithm," 14th PSCC, Sevilla, 24-28, Session 08, Paper 3, June (2002).
[5] M. Kezunovic, "Accurate Fault Location in Transmission Networks Using Modeling, Simulation and Limited Field Recorded Data," Texas A&M University, (2002).
[6] Christian Becker et al, "The influence of the series compensating FACTs devices on short - circuit behavior," university of Dortmund, Dortmund, Germany, 14th PSCC Sevilla 24-28 (Session 10 paper 1), June (2002).
[7] W. Cheong, "Wavelet analysis of the fault transient phenomena on an improved thyristor controlled series compensated transmission line model with particular reference to fault type classification," university of Bath, Bath, United Kingdom, (2002).
[8] M. Sanaye-Pasand , H. Khorashadi-Zadeh, "Transmission Line Fault Detection & Phase Selection Using ANN," International Conference on Power Systems Transients –IPST, in New Orleans, USA (2003).
[9] P.M. Anderson &S.S Fouad, "power system control & stability," vol.1, the IOWA state university press, AMES, IOWA, ,USA, (1977).
[10] A.F. Bati, "The operation of small synchronous generator with particular reference to the excitation system control," Ph.D. Thesis, London, (1988).

List of Symbols and Notations

Symbols & notations	meanings & units		subscripts	Meanings
D	damping constant		**a**	armature
E	SG terminal voltage ,volt		**d**	direct axis
i	current , Amper		**e**	transmission line
L	inductance, H		**el**	electrical
P	power ,watt		**f**	SG field coil
R	Transmission line resistance , Ω		**kd**	direct axis damping coil
r	armature resistance , Ω		**kq**	quadrature axis damping coil
V,v	Voltage , volt		**m**	magnetizing
T	torque ,Newton-Meter		**mec**	mechanical
X	reactance, Ω		**q**	quadrate axis
Z	impedance , Ω		$\mathbf{T_1}$, $\mathbf{T_2}$	power transformers 1 and 2
υ (mu)	instantaneous angular speed of rotor ,rad/sec		$\mathbf{V_\infty}$	infinite busbar voltage
τ_j	mechanical time constant ,sec			
δ				

Table (1) Training data for the ANN

	Location no.	State variables limitations (p.u)		
		i_d	i_q	υ
1	One	$< i_d < 1$ -4	$< i_q < 3$ -3	$< \upsilon < 1.2$ 0.6
2	Two	$-7 < i_d < 5$	$< i_q < 6$ -9	$< \upsilon < 1.8$ -0.2
3	Three	$-14 < i_d < 8$	$< i_q < 9$ -10	$< \upsilon < 2.1$ -0.3
4	Four	$-21 < i_d < 10$	$< i_q < 11$ -12	$< \upsilon < 2.3$ -0.35

Table (2): Expected and Actual output from the ANN

Location No.	**Expected Output**				**Actual Output**			
	location 1	**location 2**	**location 3**	**location 4**	**location 1**	**location 2**	**location 3**	**location 4**
1	**1**	**0**	**0**	**0**	**0.9974**	**0.0020**	**0.0013**	**0.0001**
2	**0**	**1**	**0**	**0**	**0.0024**	**0.9965**	**-0.001**	**0.0041**
3	**0**	**0**	**1**	**0**	**0.0017**	**0.0012**	**0.9994**	**0.0006**
4	**0**	**0**	**0**	**1**	**0.0011**	**0.0004**	**0.0022**	**0.9996**

Table (3): Inputs and Outputs of ANN fault Location

Fault Location (Km)	R_{ae} p.u	L_{de} p.u	L_{qe} p.u
10	0.02109	2.1	2.04
11.66	0.025	1.75	1.69
12.14	0.03	1.65	1.59
12.38	0.035	1.60	1.54
12.62	0.04	1.55	1.49
12.78	0.045	1.51	1.45

Table (4): Test results for fault location

Fault location (Km)	ANN output (Km)
10.00	10.005
11.66	11.656
12.14	12.131
12.38	12.371
12.62	12.612
12.78	12.805

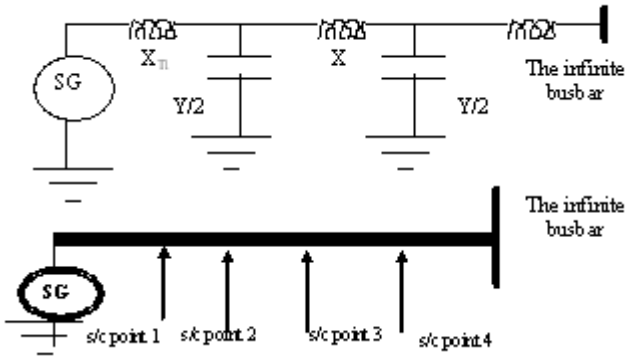

Figure (1): The simple PS model and TL trip locations

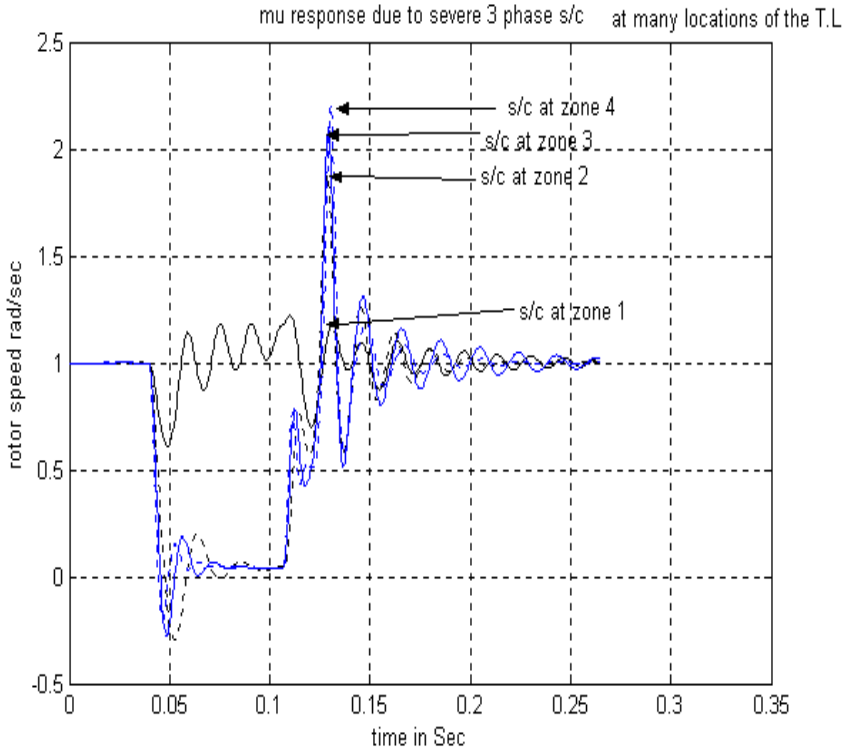

Figure (2): υ responses due to severe 3-phase s/c at many locations of the T.L

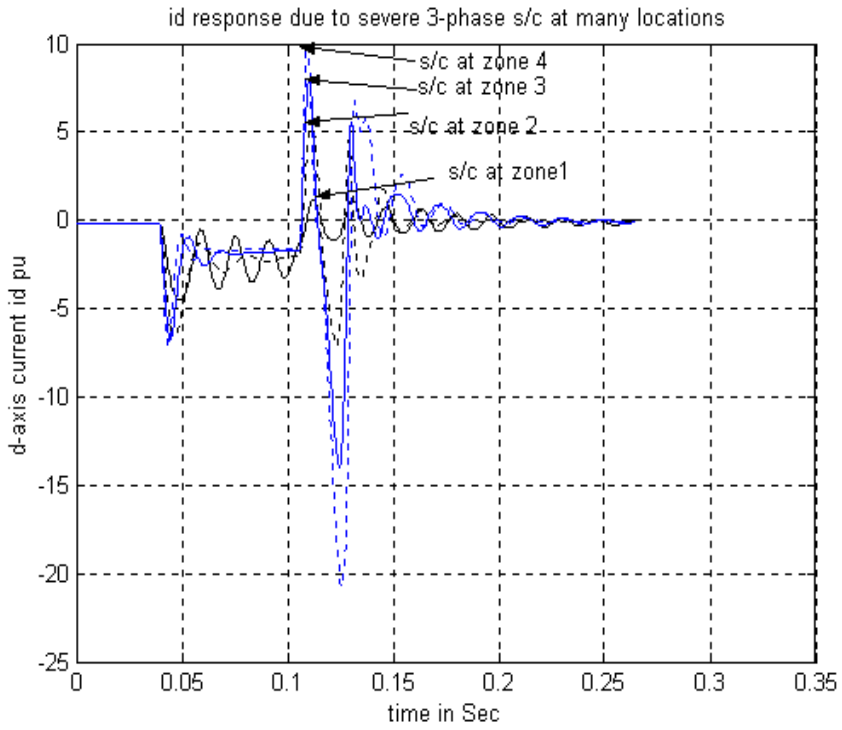

Figure (3): i_d responses due to severe 3-phase short circuit at many locations of the T.L

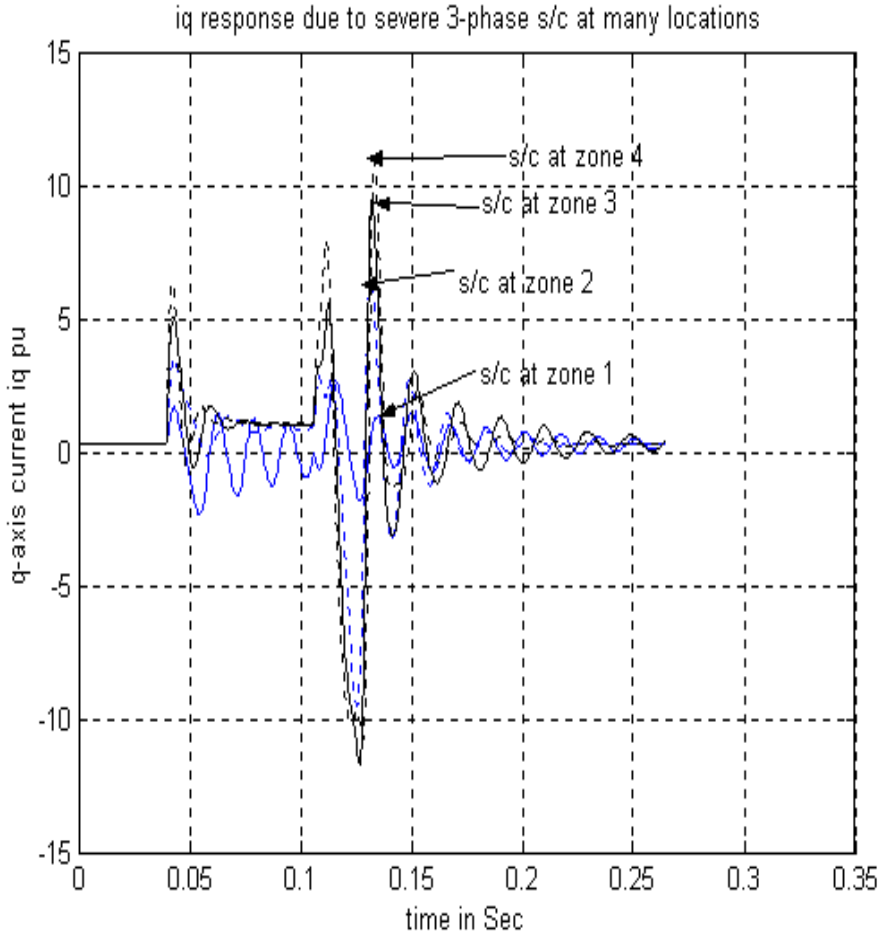

Figure (4): i_q responses due to severe 3-phase short circuit at many locations of the T.L

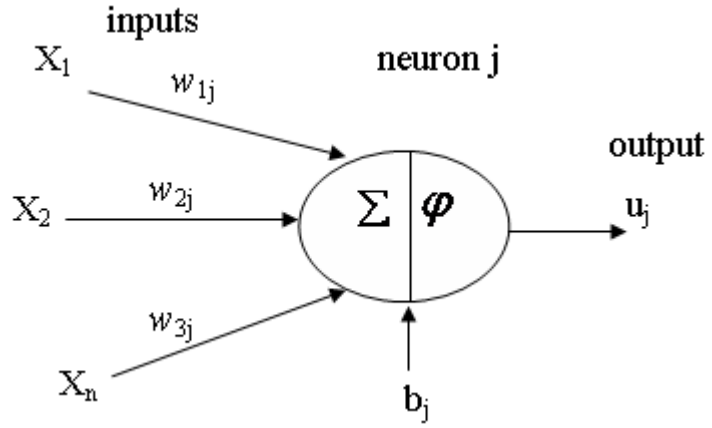

Figure (5): Information processing in a neural network unit

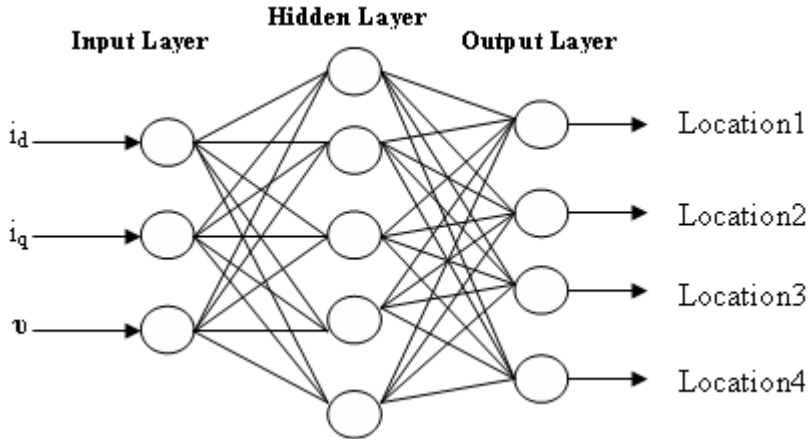

Figure (6): ANN Fault Detector Structure.

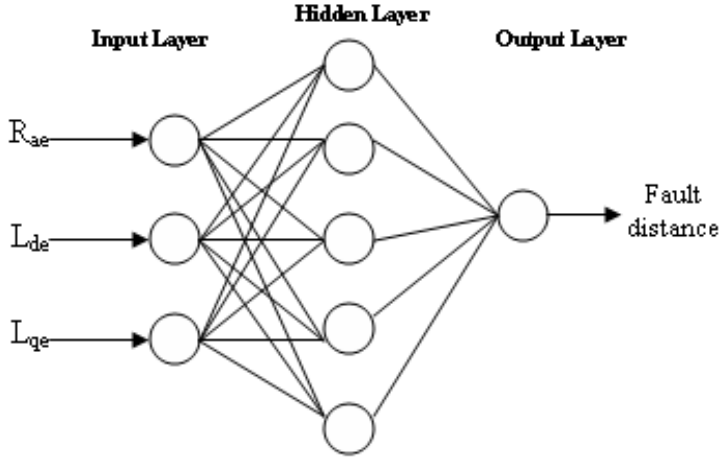

Figure (7): ANN Structure of Fault Locator.

استعمال دوائر الشبكات العصبية الاصطناعية في اكتشاف وتحديد موقع دائرة قصر شديدة (ثلاثية الأطوار) على خطوط نقل الطاقة لنظام قدرة غير مسيطر عليه

السيد منتصر عبد الواحد سلمان
ماجستير هندسة كهربائية
كلية الحاسوب – جامعة الأنبار

السيد سهيل محمد علي
ماجستير هندسة كهربائية
كلية الحاسوب – جامعة الأنبار

الخلاصة :

تم تمثيل أعطال دائرة القصر الشديدة على أربعة مواقع عشوائية من خط نقل الطاقة العائد إلى نظام قدرة غير خاضع للسيطرة . تم تسجيل استجابات ثلاثة متغيرات قابلة للقياس من متغيرات نظام القدرة (سرعة الجزء الدوار ومركبتي تيار الجزء الثابت المتعامدتان)، ثم دربت دوائر شبكات عصبية مناسبة لاكتشاف حدوث تلك الأعطال وتحديد أمكنتها. لقد برهن البحث أن هذه الطريقة هي سريعة وفعالة ودقيقة لتشخيص تلك الأعطال ومعرفة أماكنها.